Spatiotemporal coherence properties of entangled light beams generated by parametric down-conversion

Adel Joobeur and Bahaa E. A. Saleh
Department of Electrical and Computer Engineering, University of Wisconsin, Madison, Wisconsin, 53706

Malvin C. Teich
Department of Electrical Engineering, Columbia University, New York, New York 10027
(Received 28 April 1994)

We investigate the amplitude and intensity spatiotemporal coherence and the photon coincidence rates of far-field down-converted light resulting from the interaction of a pump wave of finite spectral width with a nonlinear crystal of finite spatial width. We examine the interplay between energy and phase mismatches and their effects on the intrabeam and interbeam spatial and temporal coherence of the down-converted beams. We show that the down-converted light is spatially incoherent in the second order, and that the signal-idler fourth-order coherence extends over finite entanglement angles. We also study the effect of the apertures through which the down-converted light is collected, when they are centered at phase-matched or misaligned directions.

PACS number(s): 42.50.Ar, 42.50.Dv, 42.65.Ky

I. INTRODUCTION

The process of spontaneous parametric down-conversion results in the splitting of pump photons into highly correlated photon pairs constituting an entangled "twin" state [1–6]. Conservation of energy imparts correlation to each spectral component of the signal wave and a corresponding component of the idler wave. Similarly, conservation of momentum (or phase matching) imparts correlation between pairs of directions of propagation (or spatial Fourier components) of the signal and idler beams. As a result, the two beams have unique temporal and spatial correlation properties. These correlations have been demonstrated in previous studies [7–9], associated nonclassical fourth-order interference effects have been observed [10–17], and experiments in which Bell's inequality is violated have been investigated [17,18]. Applications of the twin states to the generation of photon-number squeezed (sub-Poisson) light [19,20] and to quantum cryptography [21,22] are being vigorously pursued.

In this paper we determine the amplitude and intensity spatiotemporal correlation functions and the photon-coincidence rates of far-field down-converted light resulting from the interaction of a pump wave of finite spectral width with a nonlinear crystal of finite width. The finite spectral width of the pump offers some flexibility since there is more than one possibility for satisfying conservation of energy, and the finite width of the crystal permits some mismatch in the longitudinal components of the photon momentum. We examine the interplay between energy and phase mismatch and their effects on the spatial and temporal coherence of the down-converted light [23]. We also study the effect of transmitting and collecting the down-converted light through apertures centered at phase-matched or slightly misaligned directions.

II. QUANTUM STATE OF DOWN-CONVERTED LIGHT

Consider parametric down-conversion in a slab of material that exhibits a second-order nonlinear effect. The slab has infinite extent in the x and y directions and width l in the z direction, as depicted in Fig. 1. The pump field, treated classically, is taken to be a plane wave traveling in the z direction and described by

$$a(z,t)=\int_0^\infty d\omega_p\, A(\omega_p) e^{i[k_p z-\omega_p t]}+\text{c.c.}, \tag{1}$$

where the amplitude $A(\omega_p)$ is assumed to be a real function centered around a frequency ω_p^0.

The quadratic interaction Hamiltonian for type-I (*ooe*) parametric down-conversion, with the classical pump field assumed undepleted, is given by [6]

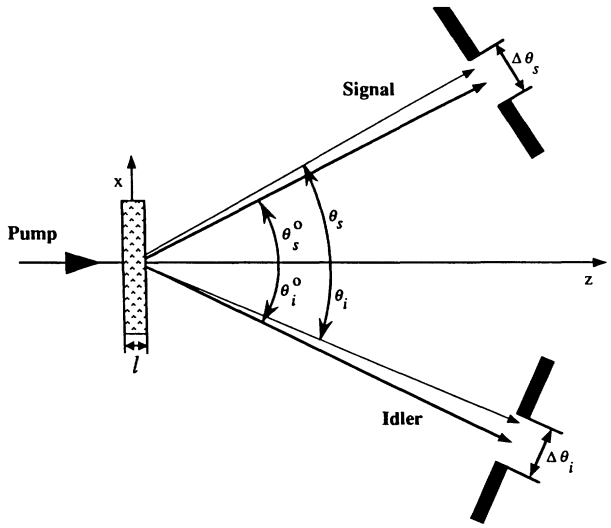

FIG. 1. Geometry of parametric down-conversion arrangement.

 ©1994 The American Physical Society

$$H_I(t)=\int_0^\infty d\omega_p \int\int d\mathbf{k}_s d\mathbf{k}_i \chi_{\text{eff}}(\omega_s,\omega_i;\omega_p) A(\omega_p) e^{i(\omega_s+\omega_i-\omega_p)t} \times \int_{-\infty}^{\infty}\int_{-\infty}^{\infty} dx\, dy \int_{-l/2}^{l/2} dz\, e^{i(\mathbf{k}_p-\mathbf{k}_s-\mathbf{k}_i)\cdot\mathbf{r}} \hat{a}^\dagger_{\mathbf{k}_s}\hat{a}^\dagger_{\mathbf{k}_i}+\text{H.c.}, \tag{2}$$

where $\hat{a}^\dagger_{\mathbf{k}_s}$ and $\hat{a}^\dagger_{\mathbf{k}_i}$ are the creation operators of the modes $\mathbf{k}_s$ and $\mathbf{k}_i$ of the signal and idler, respectively,

$$\chi_{\text{eff}}(\omega_s,\omega_i;\omega_p)=-\frac{i\omega_p^{5/2}[n_e(\omega_p)]^2(\hbar^3\omega_s\omega_i)^{1/2}}{2\pi^2c^3 n_o(\omega_s)n_o(\omega_i)}\chi^{NL}_{ijk}(\omega_s,\omega_i;\omega_p)\hat{\mathbf{e}}_i\hat{\mathbf{o}}_j(\mathbf{k}_s)\hat{\mathbf{o}}_k(\mathbf{k}_i) \tag{3}$$

is the effective susceptibility, c is the speed of light in free space, $\hat{\mathbf{e}}$ is the extraordinary polarization direction of the pump, and $\hat{\mathbf{o}}(\mathbf{k}_s)$ and $\hat{\mathbf{o}}(\mathbf{k}_i)$ are the ordinary polarization directions of the signal and idler fields. These signal and idler polarization directions are not used to label $\hat{a}^\dagger_{\mathbf{k}_s}$ and $\hat{a}^\dagger_{\mathbf{k}_i}$ because they are set by the propagation vectors $\mathbf{k}_s$ and $\mathbf{k}_i$ in the type-I phase matching assumed here. The wave vectors $\mathbf{k}_p$, $\mathbf{k}_s$, and $\mathbf{k}_i$ for the pump, signal, and idler have magnitudes $(\omega_p/c)n_e(\omega_p)$, $(\omega_s/c)n_o(\omega_s)$, and $(\omega_i/c)n_o(\omega_i)$, respectively, where $n_e(\omega_p)$ is the extraordinary refractive index at the fixed pump propagation direction $\hat{z}$, and $n_o(\omega)$ is the ordinary refractive index. Integration over x, y, and z reduces Eq. (2) to

$$H_I(t)=\int_0^\infty d\omega_p \int\int d\mathbf{k}_s d\mathbf{k}_i \chi_{\text{eff}}(\omega_s,\omega_i;\omega_p)\delta(k_{x,s}+k_{x,i})\delta(k_{y,s}+k_{y,i}) \times l\,\text{sinc}\left[\frac{1}{2\pi}(k_{z,s}+k_{z,i}-k_p)\right] A(\omega_p)e^{i(\omega_s+\omega_i-\omega_p)t}\hat{a}^\dagger_{\mathbf{k}_s}\hat{a}^\dagger_{\mathbf{k}_i}+\text{H.c.}, \tag{4}$$

where $\text{sinc}(x)\equiv\sin(\pi x)/\pi x$. This Hamiltonian is the same as that used by Hong and Mandel [6], except here we have taken the crystal to be infinite in the x and y directions and the pump to be of finite spectral width.

Assuming that the down-converted field is initially in the vacuum state to first-order approximation in the evolution operator, the state then becomes a superposition of the vacuum state and the state

$$|\text{twin}\rangle=\int_0^\infty d\omega_p \int\int d\mathbf{k}_s d\mathbf{k}_i \chi_{\text{eff}}(\omega_s,\omega_i;\omega_p)\delta(k_{x,s}+k_{x,i})\delta(k_{y,s}+k_{y,i}) \times l\,\text{sinc}\left[\frac{l}{2\pi}(k_{z,s}+k_{z,i}-k_p)\right]\delta(\omega_s+\omega_i-\omega_p)A(\omega_p)|\mathbf{k}_s\rangle_s|\mathbf{k}_i\rangle_i\,. \tag{5}$$

The first-order approximation is satisfactory when the pump field strength and the crystal width are sufficiently small so that parametric amplification is negligible. Although the presence of the vacuum state in this superposition can have physically observable effects [24], it does not play any role in the effects considered in this paper and shall be ignored.

The frequency δ function in Eq. (5), which ensures conservation of energy, is used to remove the integration over pump frequencies, whereupon the state simplifies to

$$|\text{twin}\rangle=\int\int d\mathbf{k}_s d\mathbf{k}_i \chi_{\text{eff}}(\omega_s,\omega_i;\omega_s+\omega_i)\delta(k_{x,s}+k_{x,i})\delta(k_{y,s}+k_{y,i}) \times l\,\text{sinc}\left[\frac{l}{2\pi}\{k_{z,s}+k_{z,i}-k_p(\omega_s+\omega_i)\}\right] A(\omega_s+\omega_i)|\mathbf{k}_s\rangle_s|\mathbf{k}_i\rangle_i\,. \tag{6}$$

The δ function in Eq. (6) represents conservation of transverse momentum, and implies that, for each individual down-conversion event, the directions of the pump, signal, and idler photons are coplanar [2]. The sinc function represents conservation of momentum in the longitudinal z direction, which is not precise because of the finite width l of the crystal.

To simplify Eq. (6), we need to use the remaining two δ functions to reduce the number of integrations. This is done by expanding the arguments of the functions inside the integral in Eq. (6) to first order in the signal and idler frequencies and directions.

Assume that the signal and idler beams are observed through two rectangular apertures of the same small size Δy in the y direction and of angular openings $\Delta\theta_s$ and $\Delta\theta_i$ in the x-z plane, respectively. Thus, the δ function representing conservation of momentum in the y direction will be satisfied for all pairs of signal and idler points in the signal and idler apertures. Let θ_s^0 be the angle of the central direction of the signal aperture, as shown in Fig. 1. This signal direction fixes a conjugate idler direction with angle θ_i^0. For this pair of directions, there is a pair of signal and idler wave vectors $\mathbf{k}_s^0=(n_s\omega_s^0/c)(\hat{\mathbf{x}}\sin\theta_s^0+\hat{\mathbf{z}}\cos\theta_s^0)$ and $\mathbf{k}_i^0=(n_i\omega_i^0/c)(\hat{\mathbf{x}}\sin\theta_i^0+\hat{\mathbf{z}}\cos\theta_i^0)$ that are frequency and phase matched to the central pump wave vector $\mathbf{k}_p^0=(n_p\omega_p^0/c)\hat{\mathbf{z}}$. Here, n_s and n_i are the ordinary refractive indices at the frequencies ω_s^0 and ω_i^0, respectively, and n_p is the extraordinary refractive index at the pump frequency $\omega_p^0=\omega_s^0+\omega_i^0$. In general, for a given signal direction there is more than one configuration that achieves phase and energy matching [2]. However, it is possible to specify only one configuration by the use of filters and apertures.

Now that we have selected central frequencies and central wave vectors pointing toward the centers of the selected apertures, the next step is to examine other frequencies and directions. We expand $k_{x,s}+k_{x,i}$ to first order in $\omega_s-\omega_s^0$, $\omega_i-\omega_i^0$, $\theta_s-\theta_s^0$, and $\theta_i-\theta_i^0$ and use the δ functions in Eq. (6) to solve for one of the four variables in terms of the remaining three. Solving for the idler frequency, we obtain

$$\omega_i(\omega_s,\theta_s,\theta_i)=\omega_i^0+a_1(\omega_s-\omega_s^0)+b_1(\theta_s-\theta_s^0)+c_1(\theta_i-\theta_i^0)\ , \tag{7a}$$

where

$$a_1=-\frac{N_s\sin\theta_s^0}{N_i\sin\theta_i^a}\ , \tag{7b}$$

$$b_1=-\frac{n_s\omega_s^0\cos\theta_s^0}{N_i\sin\theta_i^0}\ , \tag{7c}$$

$$c_1=-\frac{n_i\omega_i^0}{N_i}\cot\theta_i^0\ , \tag{7d}$$

and N_p, N_s, and N_i are the pump, signal, and idler group refraction indexes evaluated at the central frequencies. Using Eq. (7a) and expanding $\omega_s+\omega_i$ to first order in the frequencies and angles of the signal and the idler fields, we get

$$\Delta\omega\equiv\omega_s+\omega_i-\omega_p^0=(1+a_1)(\omega_s-\omega_s^0)+b_1(\theta_s-\theta_s^0)+c_1(\theta_i-\theta_i^0)\ . \tag{8}$$

Similarly, expanding $k_{z,s}+k_{z,i}-k_p$ we obtain

$$\Delta k_z\equiv k_{z,s}+k_{z,i}-k_p=a_2(\omega_s-\omega_s^0)+b_2(\theta_s-\theta_s^0)+c_2(\theta_i-\theta_i^0)\ , \tag{9a}$$

where

$$a_2=\frac{N_s\cos\theta_s^0-N_p}{c}+\frac{N_i\cos\theta_i^0-N_p}{c}a_1\ , \tag{9b}$$

$$b_2=-\frac{n_s\omega_s^0\sin\theta_s^0}{c}+\frac{N_i\cos\theta_i^0-N_p}{c}b_1\ , \tag{9c}$$

and

$$c_2=-\frac{n_i\omega_i^0\sin\theta_i^0}{c}+\frac{N_i\cos\theta_i^0-N_p}{c}c_1\ . \tag{9d}$$

Finally, substituting for $\Delta\omega$ and Δk_z from Eqs. (8) and (9a), and assuming that the effective susceptibility and the Jacobian, which are needed in the change of differentials from $d\mathbf{k}$ to $d\theta\,d\varphi\,d\omega$, are slowly varying functions compared to the pump amplitude and the phase-matching sinc functions, Eq. (6) simplifies to

$$|\text{twin}\rangle=N\int_0^\infty d\omega_s\int d\theta_s\int d\theta_i\,A(\omega_p^0+(1+a_1)(\omega_s-\omega_s^0)+b_1(\theta_s-\theta_s^0)+c_1(\theta_i-\theta_i^0))\times\text{sinc}\left[\frac{l}{2\pi}\{a_2(\omega_s-\omega_s^0)+b_2(\theta_s-\theta_s^0)+c_2(\theta_i-\theta_i^0)\}\right]|\theta_s,\omega_s\rangle_s|\theta_i,\omega_i(\omega_s,\theta_s,\theta_i)\rangle_i\ , \tag{10}$$

where N is a normalization constant. In Eq. (10), we have replaced the ket $|\mathbf{k}_s\rangle_s|\mathbf{k}_i\rangle_i$ with the ket $|\theta_s,\omega_s\rangle_s|\theta_i,\omega_i(\omega_s,\theta_s,\theta_i)\rangle_i$, where $\omega_i(\omega_s,\theta_s,\theta_i)$ is given by Eq. (7a) to indicate that the independent degrees of freedom in this expansion are the angles θ_s and θ_i and the signal frequency ω_s. It is clear from Eq. (10) that the twin state cannot be factored into a product of signal and idler states and that the three quantities, θ_s, θ_i, and ω_s, are linked together through the pump spectral distribution function $A(\omega)$ and the sinc function representing approximate longitudinal phase matching.

In Eq. (10), the signal and idler directions and the signal frequency are taken as independent variables. This emphasis of propagation directions over frequencies will prove useful when calculating the coincidence rates of photons passing through a pair of apertures. However, in other situations it will be more useful to emphasize frequencies over propagation directions. Solving for the idler direction instead of the idler frequency in Eqs. (7a) and (9a), the twin state has the equivalent form

$$|\text{twin}\rangle=N\int_0^\infty d\omega_s\int_0^\infty d\omega_i\int d\theta_s\,\text{sinc}\left[\frac{l}{2\pi}\{a(\omega_s-\omega_s^0)+b(\omega_i-\omega_i^0)+c(\theta_s-\theta_s^0)\}\right]\times A(\omega_p^0+(\omega_s-\omega_s^0)+(\omega_i-\omega_i^0))|\omega_s,\theta_s\rangle_s|\omega_i,\theta_i(\omega_s,\omega_i,\theta_s)\rangle_i\ , \tag{11}$$

where a, b, and c can be obtained from Eqs. (7a) and (9a).

The signal and idler wave-vector pairs for which the weighting function under the integral in Eqs. (10) or (11) is maximum are determined by setting $\Delta\omega=0$ and $\Delta k_z=0$. In the limit of infinite crystal width l and a monochromatic pump [whereupon the function $A(\omega)$ and the sinc function in Eqs. (10) or (11) are replaced by δ functions), these wave vectors become the only interacting pairs. In this case, for a given signal direction θ_s, it will generally be possible to solve uniquely for θ_i, ω_s, and ω_i using $\Delta\omega=0$, $\Delta k_z=0$, and Eq. (7a), which represents the linear approximation of the intersection of the matching surface and the x-z plane around the angle θ_s^0, to obtain

$$|\text{twin}\rangle = N\int d\theta_s |\theta_s, \omega_s(\theta_s)\rangle_s |\theta_i(\theta_s), \omega_i(\theta_s)\rangle_i \ . \quad (12)$$

It follows that at a given signal or idler direction the field is monochromatic and that a given single direction is matched with only one idler direction. In contrast, when the pump has a finite spectral width and the crystal is finite in width, the field in a given signal or idler direction is spectrally broadened and a given signal direction is matched with a cone of idler directions of order $\Delta\theta_i^c$, as illustrated in Fig. 2.

It is useful to compare our expression for the twin state with the phenomenological expression used by Campos, Saleh, and Teich [25],

$$|\text{twin}\rangle = \int_0^\infty \int_0^\infty \zeta(\omega_s, \omega_i) |\omega_s\rangle_s |\omega_i\rangle_i d\omega_s d\omega_i \ , \quad (13)$$

where $|\zeta(\omega_s, \omega_i)|^2$ is a joint Gaussian function. This expression can be obtained from Eq. (11) by making few reasonable assumptions and approximations. First, we assume exact phase matching by replacing the sinc function in Eq. (11) with a δ function, and thereby obtain

$$|\text{twin}\rangle = N\int\int d\omega_s d\omega_i A(\omega_p^0 + (\omega_s - \omega_s^0) + (\omega_i - \omega_i^0)) |\omega_s, \theta_s(\omega_s, \omega_i)\rangle_s |\omega_i, \theta_i(\omega_s, \omega_i)\rangle_i \ , \quad (14)$$

where, in this case, both θ_s and θ_i are determined uniquely for each frequency pair. This expression takes the same form as the state described by Eq. (13) if

$$\zeta(\omega_s, \omega_i) = NA(\omega_p^0 + (\omega_s - \omega_s^0) + (\omega_i - \omega_i^0)) \ , \quad (15)$$

and the angles in the kets in Eq. (14) are ignored, which is appropriate as long as these directions lie within the collection apertures and the observables of interest do not resolve directions within these collection apertures.

For a pump field with a normalized Gaussian amplitude distribution,

$$A(\omega_p) = (2\pi\Delta\omega_p^2)^{-1/4} \exp\left\{-\left[\frac{\omega_p - \omega_p^0}{2\Delta\omega_p}\right]^2\right\} , \quad (16)$$

Eq. (15) becomes

$$\zeta(\omega_s, \omega_i) \propto \exp\left\{-\left|\frac{(\omega_s - \omega_s^0) + (\omega_i - \omega_i^0)}{2\Delta\omega_p}\right|^2\right\} . \quad (17)$$

The amplitude $\zeta(\omega_s, \omega_i)$ given by this last equation is constant for the family of straight lines $(\omega_s - \omega_s^0) + (\omega_i + \omega_i^0) = \text{const}$. At frequencies for which ω_s or ω_i deviate significantly from their central values, the linear expansions of $\Delta\omega$ and Δk_z fail but apertures (or possible filters) will in general limit the deviation to the appropriate range.

To incorporate these elements we modify Eq. (17) to

$$\zeta(\omega_s, \omega_i) = A_0 \exp\left\{-\left|\frac{(\omega_s - \omega_s^0) + (\omega_i - \omega_i^0)}{2\Delta\omega_p}\right|^2\right\} \times t_s(\omega_s) t_i(\omega_i) \ , \quad (18)$$

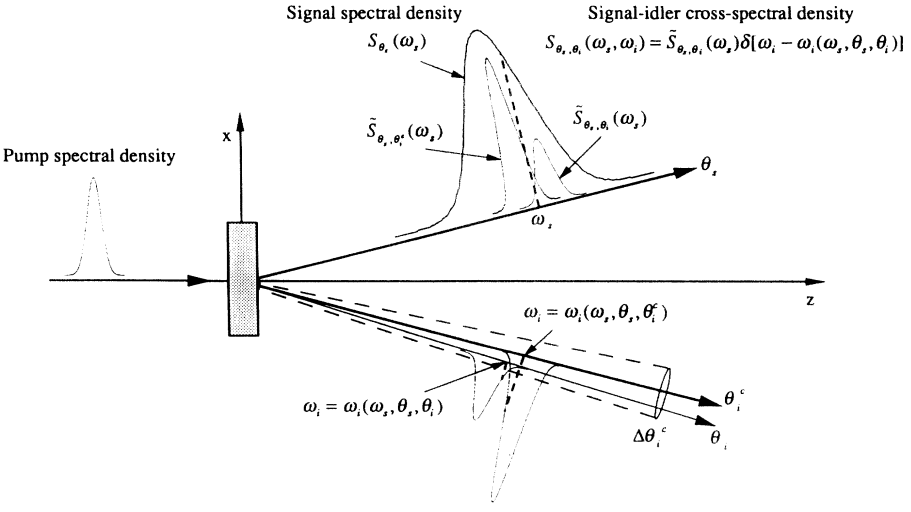

FIG. 2. Illustration of the signal spectral density and signal-idler cross-spectral density. Contributions to the signal spectral density $S_{\theta_s}(\omega_s)$ from the matched idler angle θ_i^c and from another idler angle θ_i within the idler entanglement angle $\Delta\theta_i^c$ are shown. The signal-idler cross-spectral density $S_{\theta_s,\theta_i}(\omega_s, \omega_i)$ between the pair of signal and idler directions θ_s and θ_i is given by the product of $\tilde{S}_{\theta_s,\theta_i}(\omega_s)$ and $\delta(\omega_i - \{\omega_i^0 + a_1(\omega_s - \omega_s^0) + b_1(\theta_s - \theta_s^0) + c_1(\theta_i - \theta_i^0)\})$.

where $t_s(\omega_s)$ and $t_i(\omega_i)$ are the normalized transmittances of the signal and idler channels, respectively, and A_0 is a normalization constant. Assuming

$$t_s(\omega_s)=(2\pi\Delta\omega_1^2)^{-1/4}\exp\left\{-\left[\frac{(\omega_s-\omega_s^0)}{2\Delta\omega_1}\right]^2\right\}, \quad (19a)$$

and

$$t_i(\omega_i)=(2\pi\Delta\omega_1^2)^{-1/4}\exp\left\{-\left[\frac{(\omega_i-\omega_i^0)}{2\Delta\omega_1}\right]^2\right\}, \quad (19b)$$

the amplitude $\zeta(\omega_s,\omega_i)$ becomes

$$\zeta(\omega_s,\omega_i)=(2\pi\sigma^2)^{-1/2}(1-\eta^2)^{-1/4}\times\exp\left[-\frac{(\omega_s-\omega_s^0)^2+(\omega_i-\omega_i^0)^2-2\eta(\omega_s-\omega_s^0)(\omega_i-\omega_i^0)}{4(1-\eta^2)\sigma^2}\right], \quad (20a)$$

where

$$\eta=-\frac{\Delta\omega_1^2}{\Delta\omega_1^2+\Delta\omega_p^2}, \quad (20b)$$

and

$$\sigma=\Delta\omega_1\left[\frac{\Delta\omega_1^2+\Delta\omega_p^2}{2\Delta\omega_1^2+\Delta\omega_p^2}\right]^{1/2}. \quad (20c)$$

The actual frequency width $\Delta\omega_1$ is determined by the apertures and filters that are employed; it is assumed here to be the same for both the signal and idler channels. Thus the contours of constant $\zeta(\omega_s,\omega_i)$ are now ellipses instead of straight lines and the jointly Gaussian state used by Campos, Saleh, and Teich is reproduced. A fully correlated state with $\eta=-1$ is obtained in the limit as $\Delta\omega_1/\Delta\omega_p\to\infty$, in which case $\sigma\to\Delta\omega_1/\sqrt{2}$.

III. COHERENCE FUNCTIONS AND COINCIDENCE RATES

In this section, expressions for the second-order (amplitude) and fourth-order (intensity) coherence functions for the signal and idler fields of the down-converted light are determined. In the far-field approximation, only modes with propagation vectors in the observation direction contribute to the field at a given observation point, so that the positive-frequency part of the electric-field operator is given by [26]

$$\hat{E}^+(\mathbf{r},t)=\frac{1}{c^2 r}\left[\frac{\hbar}{V}\right]^{1/2}\int_0^\infty d\omega\,\omega^{3/2}e^{i\omega[(r/c)-t]}\hat{a}_{\mathbf{k}}, \quad (21)$$

where $\mathbf{k}=(\omega/c)\hat{\mathbf{r}}$, $\mathbf{r}$ is the position vector from the source to the observation point, and V is the normalization volume. It is more convenient to work with the signal- and idler-field operators

$$\hat{V}_s^+(\theta_s,r,t)=\int_0^\infty d\omega_s e^{i\omega_s[(r/c)-t]}\hat{a}_{\theta_s,\omega_s}, \quad (22a)$$

and

$$\hat{V}_i^+(\theta_i,r,t)=\int_0^\infty d\omega_i e^{i\omega_i[(r/c)-t]}\hat{a}_{\theta_i,\omega_i}, \quad (22b)$$

which are defined such that the operator $\hat{V}^-\hat{V}^+$ has the dimensions of photon density [27] and where the frequency dependency of the field operators is absorbed in the susceptibility [6]. The creation and annihilation operators obey the commutation relations

$$[\hat{a}_{\theta_s,\omega_s},\hat{a}^\dagger_{\theta_s',\omega_s'}]=\delta(\theta_s-\theta_s')\delta(\omega_s-\omega_s'), \quad (23a)$$

$$[\hat{a}_{\theta_i,\omega_i},\hat{a}^\dagger_{\theta_i',\omega_i'}]=\delta(\theta_i-\theta_i')\delta(\omega_i-\omega_i'), \quad (23b)$$

and all other commutators are zero.

The results obtained so far have been for a single pump wave packet. We now consider a superposition of a sequence of such wave packets arriving at statistically independent random times $\{t_m\}$ constituting a stationary (homogeneous) Poisson point process [28]. Thus

$$E_p(z,t)=\sum_m a(z,t-t_m)+\text{c.c.}, \quad (24a)$$

where

$$a(z,t)=\int_0^\infty d\omega\,A(\omega)e^{i[kz-\omega t]}. \quad (24b)$$

The resulting second- and fourth-order coherence functions obtained by averaging over the random times $\{t_n\}$ are also applicable to a cw laser pump of a finite spectral width modeled as a sequence of such wave packets as long as the parametric down-conversion is spontaneous [1,29–31] so that there is no constant phase relation between different photon pair emissions. To simplify the derivation of the second- and fourth-order coherence functions, we further assume that the rate of twin-photon emissions μ is sufficiently low so that the resulting down-converted wave packets rarely overlap.

The down-converted light is then described by a random sequence of twin states $\{|\text{twin};t_n\rangle\}$, where $\{t_n\}$ is a randomly deleted version of the pump sequence $\{t_m\}$, which is also a Poisson point process [28]. The result analogous to Eq. (10) is then

$$|\text{twin};t_n\rangle = N\int_0^\infty d\omega_s \int d\theta_s \int d\theta_i \exp i\{[\omega_p^0+(1+a_1)(\omega_s-\omega_s^0)+b_1(\theta_s-\theta_s^0)+c_1(\theta_i-\theta_i^0)]t_n\}$$
$$\times A(\omega_p^0+(1+a_1)(\omega_s-\omega_s^0)+b_1(\theta_s-\theta_s^0)+c_1(\theta_i-\theta_i^0))$$
$$\times \operatorname{sinc}\left[\frac{l}{2\pi}\{a_2(\omega_s-\omega_s^0)+b_2(\theta_s-\theta_s^0)+c_2(\theta_i-\theta_i^0)\}\right]$$
$$\times |\theta_s,\omega_s\rangle_s |\theta_i,\omega_i(\omega_s,\theta_s,\theta_i)\rangle_i \ . \tag{25}$$

This description of the down-converted light as a random sequence of twin states is similar to the model employed by Teich, Saleh, and Perina [28]. Here we incorporate the random emission times in the states instead of the field operators. Also, as a result of the assumption that the wave packets do not overlap, the derivation is much simpler because of the lack of interpacket interference.

A. Second-order coherence functions

1. *Signal-idler mutual coherence function*

The second-order (or amplitude) coherence function of the down-converted field at a point of the signal beam and at another of the idler beam is given by

$$G_{si}^{(1)}(\theta_s,\theta_i;\tau) = \sum_n \overline{\langle \text{twin};t_n|\hat{V}_s^-(\theta_s,t)\hat{V}_i^+(\theta_i,t+\tau)|\text{twin};t_n\rangle}$$
$$= \mu\int dt_n \langle \text{twin};t_n|\hat{V}_s^-(\theta_s,t)\hat{V}_i^+(\theta_i,t+\tau)|\text{twin};t_n\rangle \ , \tag{26}$$

where the bar indicates averaging over the random times $\{t_n\}$. Contributions from pairs of different wave packets have been neglected since these packets rarely overlap. This expected value vanishes because of the single-photon nature of the constituent beams in the twin state, so that

$$G_{si}^{(1)}(\theta_s,\theta_i;\tau) = 0 \ . \tag{27}$$

This means that it is not possible to see second-order interference effects by superimposing the signal and idler beams. This is not the case with the fourth-order coherence function [17], as will be shortly seen.

2. *Signal coherence function*

The second-order coherence function at pairs of points within the signal field is

$$G_{ss}^{(1)}(\theta_s,\theta_s';\tau) = \mu\int dt_n \langle \text{twin};t_n|\hat{V}_s^-(\theta_s,t)\hat{V}_s^+(\theta_s',t+\tau)|\text{twin};t_n\rangle$$
$$= \mu\int dt_n N^2 \int d\omega_s' d\phi_s' d\phi_i' \int d\omega_s d\phi_s d\phi_i \int d\omega\, d\omega' e^{-i\omega'(r/c-t)} e^{i\omega(r/c-t-\tau)}$$
$$\times e^{-i[\omega_p^0+\Delta\omega']t_n} A(\omega_p^0+\Delta\omega')\operatorname{sinc}\left[\frac{l}{2\pi}\Delta k_z'\right] e^{i[\omega_p^0+\Delta\omega]t_n} A(\omega_p^0+\Delta\omega)\operatorname{sinc}\left[\frac{l}{2\pi}\Delta k_z\right]$$
$$\times {}_i\langle \phi_i',\omega_i(\omega_s',\phi_s',\phi_i')|_s\langle \phi_s',\omega_s'|\hat{a}^\dagger_{\theta_s',\omega'}\hat{a}_{\theta_s,\omega}|\phi_s,\omega_s\rangle_s|\phi_i,\omega_i(\omega_s,\phi_s,\phi_i)\rangle_i \ , \tag{28}$$

where $\Delta\omega$ and Δk_z are functions of $(\omega_s,\theta_s,\phi_i)$ and $\Delta\omega'$ and $\Delta k_z'$ are functions of $(\omega_s',\phi_s',\phi_i')$, as provided in Eqs. (8) and (9a). Noting that the integrand in Eq. (28) is proportional to

$$\delta(\phi_s-\theta_s)\delta(\phi_s'-\theta_s')\delta(\phi_i-\phi_s')\delta(\omega_s-\omega)\delta(\omega_s'-\omega')\delta(\omega_i(\omega_s',\phi_s',\phi_i')-\omega_i(\omega_s,\phi_s,\phi_i)) \ ,$$

and using the linear expansion of the idler frequencies given in Eq. (7a), we get

$$G_{ss}^{(1)}(\theta_s,\theta_s';\tau) = \mu\int dt_n N^2 \int d\phi_i \int d\omega\, d\omega' \delta(a_1(\omega-\omega')+b_1(\theta_s-\theta_s'))A(\omega_p^0+\Delta\omega')A(\omega_p^0+\Delta\omega)$$
$$\times \operatorname{sinc}\left[\frac{l}{2\pi}\Delta k_z'\right]\operatorname{sinc}\left[\frac{l}{2\pi}\Delta k_z\right] e^{i(\omega-\omega')(r/c-t)}$$
$$\times \exp i\{[(1+a_1)(\omega-\omega')+b_1(\theta_s-\theta_s')]t_n\} e^{-i\omega\tau} \ . \tag{29}$$

Integrating over the remaining δ function in Eq. (29), we get

$$G_{ss}^{(1)}(\theta_s,\theta_s';\tau) = \mu\int dt_n N^2 \int d\phi_i \int d\omega\ A(\omega_p^0+\Delta\omega')A(\omega_p^0+\Delta\omega)$$
$$\times \operatorname{sinc}\left[\frac{l}{2\pi}\Delta k_z'\right]\operatorname{sinc}\left[\frac{l}{2\pi}\Delta k_z\right] e^{-i[b_1(\theta_s-\theta_s')/a_1](r/c-t+t_n)} e^{-i\omega\tau} \ , \tag{30}$$

where $\Delta\omega$ and the Δk_z are functions of $(\omega_s,\theta_s,\phi_i)$ as in Eq. (28), but $\Delta\omega'$ and $\Delta k_z'$ are now functions of $(\omega_s,\theta_s,\theta_s',\phi_i)$ as determined by Eqs. (8) and (9a) and the δ function in Eq. (29). Finally, integrating over t_n to get the time average gives

$$G_{ss}^{(1)}(\theta_s,\theta_s';\tau)=\mu N^2\delta(\theta_s-\theta_s')\int_0^\infty d\omega_s e^{-i\omega_s\tau}\int d\theta_i \mathrm{sinc}^2\left[\frac{l}{2\pi}\{a_2(\omega_s-\omega_s^0)+b_2(\theta_s-\theta_s^0)+c_2(\theta_i-\theta_i^0)\}\right]$$
$$\times A^2(\omega_p^0+(1+a_1)(\omega_s-\omega_s^0)+b_1(\theta_s-\theta_s^0)+c_1(\theta_i-\theta_i^0)) . \quad (31)$$

From Eq. (31), we see that the signal light fluctuations in different directions are completely uncorrelated, so that the signal light is spatially incoherent.

3. *Signal power spectral density*

The signal light in the direction θ_s, neglecting the small contribution from the lower limit of the frequency integral in Eq. (31), has a power spectral density given by the Fourier transform of Eq. (31), i.e.,

$$S_{\theta_s}(\omega_s)=\mu N^2\int d\theta_i \mathrm{sinc}^2\left[\frac{l}{2\pi}\{a_2(\omega_s-\omega_s^0)+b_2(\theta_s-\theta_s^0)+c_2(\theta_i-\theta_i^0)\}\right]$$
$$\times A^2(\omega_p^0+(1+a_1)(\omega_s-\omega_s^0)+b_1(\theta_s-\theta_s^0)+c_1(\theta_i-\theta_i^0)) . \quad (32)$$

The result is a superposition of terms corresponding to different idler directions with weights determined by the phase mismatch and the pump power spectrum (see Fig. 2).

In the limit where the spectral width of the pump is much broader than the sinc function in Eq. (32), the sinc function can be approximated by a δ function, and Eq. (32) simplifies to

$$S_{\theta_s}(\omega_s)=\mu N^2 A^2\left[\omega_p^0+\left[1+a_1-\frac{a_2c_1}{c_2}\right](\omega_s-\omega_s^0)+\left[b_1-\frac{b_2c_1}{c_2}\right](\theta_s-\theta_s^0)\right] . \quad (33)$$

In the opposite limit, where the pump spectral distribution is much narrower than the sinc function, the pump can be taken to be monochromatic, and Eq. (32) simplifies to

$$S_{\theta_s}(\omega_s)=\mu N^2\mathrm{sinc}^2\left[\frac{\omega_s-\bar{\omega}_s}{\Delta\omega_{\theta_s}}\right] . \quad (34a)$$

Here

$$\bar{\omega}_s=\omega_s^0-\frac{c_1b_2-c_2b_1}{c_1a_2-c_2(1+a_1)}(\theta_s-\theta_s^0) \quad (34b)$$

represents the shift in the central frequency of the signal as a function of the observation direction, and

$$\Delta\omega_s=\frac{2\pi|c_1|}{|c_1a_2-c_2(1+a_1)|l} \quad (34c)$$

is a measure of the signal bandwidth in a fixed direction (which is independent of the observation direction in the linear approximation of the matching relations used here).

For the Gaussian pump power spectrum given by Eq. (16), the signal power spectrum in Eq. (32) is

$$S_{\theta_s}(\omega_s)=\mu N^2\int d\theta_i \exp\left[-\frac{\{\omega_s-\bar{\omega}_1(\theta_s,\theta_i)\}^2}{2\sigma_1^2}\right]$$
$$\times\mathrm{sinc}^2\left[\frac{\omega_s-\bar{\omega}_2(\theta_s,\theta_i)}{\sigma_2}\right] , \quad (35a)$$

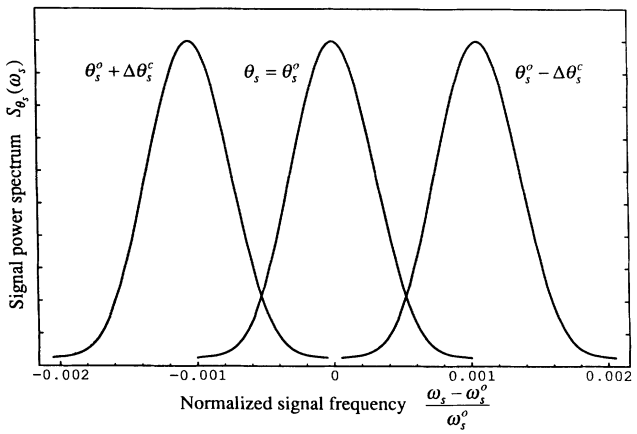

FIG. 3. Signal power spectral density $S_{\theta_s}(\omega_s)$ for different observation directions. Data approximating the experiment of Larchuk *et al.* [16] are used. A deuterated potassium dihydrogen phosphate (KD*P) crystal of width $l=15$ mm, oriented for type-I (*ooe*) phase matching at 90° incidence to the crystal's optic axis is pumped by a beam centered at $\omega_p^0=4.6316\times10^{15}$ rad/s. Nondegenerate signal and idler fields centered at $\omega_s^0=2.2600\times10^{15}$ rad/s and $\omega_i^0=2.3716\times10^{15}$ rad/s are observed. The refractive indexes [32] are $n_p=1.47675$ (extraordinary), $n_s=1.49758$ (ordinary), and $n_i=1.49847$ (ordinary). The central signal and idler angles determined from the phase-matching equations are $\theta_s^0=9.911°$ and $\theta_i^0=-9.434°$. The group refractive indexes were estimated from the dispersion formulas in Ref. [32] to be $N_p=1.51786$, $N_s=1.51739$, and $N_i=1.51831$. To have energy mismatch [width of the Gaussian function in Eq. (35a)] and phase mismatch [width of the sinc function in Eq. (35a)] of the same order, a pump frequency width $\Delta\omega_p=6\pi\times10^{11}$ rad/s was used. From these data we calculated $\Delta\omega_s=1.172\times10^{12}$ rad/s.

where

$$\bar{\omega}_1(\theta_s,\theta_i)=\omega_s^0-\frac{b_1}{1+a_1}(\theta_s-\theta_s^0)-\frac{c_1}{1+a_1}(\theta_i-\theta_i^0)\ , \tag{35b}$$

$$\bar{\omega}_2(\theta_s,\theta_i)=\omega_s^0-\frac{b_2}{a_2}(\theta_s-\theta_s^0)-\frac{c_2}{a_2}(\theta_i-\theta_i^0)\ , \tag{35c}$$

$$\sigma_1=\frac{\Delta\omega_p}{1+a_1}\ , \tag{35d}$$

and

$$\sigma_2=\frac{2\pi}{a_2 l}\ . \tag{35e}$$

The idler direction θ_i^c that matches a given signal direction θ_s is given by

$$\theta_i^c=\frac{b_2(1+a_1)-b_1a_2}{c_1a_2-c_2(1+a_1)}(\theta_s-\theta_s^0)+\theta_i^0\ , \tag{36}$$

and is obtained from the equation $\bar{\omega}_1(\theta_s,\theta_i)=\bar{\omega}_2(\theta_s,\theta_i)$.

The signal power spectrum in the given direction θ_s is maximum at the signal frequency

$$\bar{\omega}_s=\omega_s^0-\frac{b_2c_1-b_1c_2}{c_1a_2-c_2(1+a_1)}(\theta_s-\theta_s^0)\ , \tag{37}$$

which corresponds to the signal wave vector that is phase and energy matched to the corresponding wave vector in the conjugate idler direction θ_i^c. This last equation gives, to first order in the signal direction, the shift in the central frequency of the signal power spectrum as a function of the observation direction. This shift is the same as for the monochromatic pump given by Eq. (34b), which is expected since both shifts depend only on the dispersion properties of the crystal. The spectral bandwidth for a given signal direction is

$$\Delta\omega_s\equiv|\omega_{+-}-\omega_{-+}|=\frac{\left|c_2\Delta\omega_p+c_1\frac{2\pi}{l}\right|}{|c_1a_2-c_2(1+a_1)|}\ , \tag{38}$$

where ω_{+-} and ω_{-+} are solutions to $\bar{\omega}_1(\theta_s,\theta_i)\pm\Delta\omega_p/(1+a_1)=\bar{\omega}_2(\theta_s,\theta_i)\pm 2\pi/a_2 l$.

As an example, the signal power spectrum in Eq. (35a) is calculated for a particular nondegenerate down-conversion experiment and the results are shown in Fig. 3. The shift in the power spectrum peak depends on the dispersion property [32] of the crystal, but the signal spectral width depends on both the crystal parameters and the pump spectral distribution width. In this example, the pump spectral width was chosen such that $c_2\Delta\omega_p$ and $c_1(2\pi/l)$ are of the same order.

The bandwidth in Eq. (38) reduces to that in Eq. (34c) in the limiting case of $\Delta\omega_p=0$. In the other limiting case of exact phase matching, using Eq. (33) and the Gaussian pump assumption, the signal power spectrum is given by

$$S_{\theta_s}(\omega_s)=2\pi\mu N^2 e^{-(\omega_s-\bar{\omega}_s)^2/2\Delta\omega_s^2}\ , \tag{39a}$$

where $\bar{\omega}_s$ is given by Eq. (37) and

$$\Delta\omega_s=\frac{|c_2|\Delta\omega_p}{|(1+a_1)c_2-c_1a_2|} \tag{39b}$$

is the limit of Eq. (38) for $l\to\infty$.

B. Fourth-order coherence functions

Now consider the fourth-order (intensity) coherence functions at pairs of directions within one beam and across the two beams.

1. *Signal coherence function*

The fourth-order (intensity) coherence function of the signal beam, normalized to the coincidence rate, for a time delay τ sufficiently small so that the time t and $t+\tau$ lie within one pump wave packet, is given by

$$G_{ss}^{(2)}(\theta_s,\theta_s';\tau)=\mu\int dt_n\langle\text{twin};t_n|\hat{V}_s^-(\theta_s,t)\hat{V}_s^-(\theta_s',t+\tau)\hat{V}_s^+(\theta_s',t+\tau)\hat{V}_s^+(\theta_s,t)|\text{twin};t_n\rangle\ . \tag{40}$$

This expected value vanishes since the state of the down-converted light is such that only one photon exists in the signal wave packet. For τ sufficiently long, however, as a result of contributions from the overlapping wave packets the intensity correlation approaches the product $I_s(\theta_s)I_s(\theta_s')$, which represents the random coincidence rate between photons of the various wave packets. Similar results are applicable for the idler wave.

2. *Signal-idler coherence function*

The intensity correlation function for the signal and idler beams, at time delays τ sufficiently small so that the times t and $t+\tau$ lie within one pump wave packet, is given by

$$G_{si}^{(2)}(\theta_s,\theta_i;\tau)=\mu\int dt_n\langle\text{twin};t_n|\hat{V}_s^-(\theta_s,t)\hat{V}_i^-(\theta_i,t+\tau)\hat{V}_i^+(\theta_i,t+\tau)\hat{V}_s^+(\theta_s,t)|\text{twin};t_n\rangle\ . \tag{41}$$

This function represents the coincidence rates of the signal and idler photons. For τ sufficiently long, the intensity correlation approaches the product $I_s(\theta_s)I_i(\theta_i)$, which represents the rate of random coincidences between photons from the various wave packets. This rate will be much smaller than the rate given by Eq. (41) for small τ, and will be ignored.

Using Eq. (25) for the twin state, and Eqs. (22a) and (22b) for the positive-frequency parts of the signal and idler fields

and their Hermitian conjugates for the negative parts of the fields, Eq. (41) becomes

$$G_{si}^{(2)}(\theta_s,\theta_i;\tau)=\mu\int dt_n N^2\int d\omega_s' d\phi_s' d\phi_i'\int d\omega_s d\phi_s d\phi_i\int d\omega\, d\omega'\int d\omega'' d\omega'''$$
$$\times A(\omega_p^0+\Delta\omega')A(\omega_p^0+\Delta\omega)\text{sinc}\left[\frac{l}{2\pi}\Delta k_z'\right]\text{sinc}\left[\frac{l}{2\pi}\Delta k_z\right]e^{i[\omega_p^0+\Delta\omega]t_n}e^{-i[\omega_p^0+\Delta\omega']t_n}$$
$$\times e^{i(\omega/c)(r_s-ct)}e^{-i(\omega'/c)(r_s-ct)}e^{i(\omega''/c)(r_i-ct-c\tau)}e^{-i(\omega'''/c)(r_i-ct-c\tau)}$$
$$\times{}_i\langle\phi_i',\omega_i(\omega_s',\phi_s',\phi_i')|_s\langle\phi_s',\omega_s'|\hat{a}^\dagger_{\theta_s;\omega'}\hat{a}^\dagger_{\theta_i;\omega''}\hat{a}_{\theta_i;\omega'''}\hat{a}_{\theta_s;\omega}|\phi_s,\omega_s\rangle_s|\phi_i,\omega_i(\omega_s,\phi_s,\phi_i)\rangle_i\ . \tag{42}$$

Since the integrand in Eq. (42) is proportional to the δ function,

$$\delta(\phi_i'-\theta_i)\delta(\omega_i(\omega_s',\phi_s',\phi_i')-\omega''')\delta(\phi_s'-\theta_s)\delta(\omega_s'-\omega')\delta(\phi_s-\theta_s)\delta(\phi_i-\theta_i)\delta(\omega_s-\omega)\delta(\omega_i(\omega_s,\phi_s,\phi_i)-\omega'')\ ,$$

Eq. (42) simplifies to

$$G_{si}^{(2)}(\theta_s,\theta_i;\tau)=\mu\int dt_n N^2\int d\omega_s d\omega_s' e^{i(1+a_1)(\omega_s-\omega_s')t_n}e^{i(\omega_s-\omega_s')[(r_s/c)-t]}e^{ia_1(\omega_s-\omega_s')[(r_i/c)-t-\tau]}$$
$$\times A(\omega_p^0+\Delta\omega')A(\omega_p^0+\Delta\omega)\text{sinc}\left[\frac{l}{2\pi}\Delta k_z'\right]\text{sinc}\left[\frac{l}{2\pi}\Delta k_z\right]\ , \tag{43}$$

where $\Delta\omega$ and Δk_z are functions of $(\omega_s,\theta_s,\theta_i)$, and $\Delta\omega'$ and $\Delta k_z'$ are functions of $(\omega_s',\theta_s,\theta_i)$ as given by Eqs. (8) and (9a).

Performing the time averaging, we obtain

$$G_{si}^{(2)}(\theta_s,\theta_i;\tau)=\mu N^2\int_0^\infty d\omega_s\,\text{sinc}^2\left[\frac{l}{2\pi}\{a_2(\omega_s-\omega_s^0)+b_2(\theta_s-\theta_s^0)+c_2(\theta_i-\theta_i^0)\}\right]$$
$$\times A^2(\omega_p^0+(1+a_1)(\omega_s-\omega_s^0)+b_1(\theta_s-\theta_s^0)+c_1(\theta_i-\theta_i^0))\ , \tag{44}$$

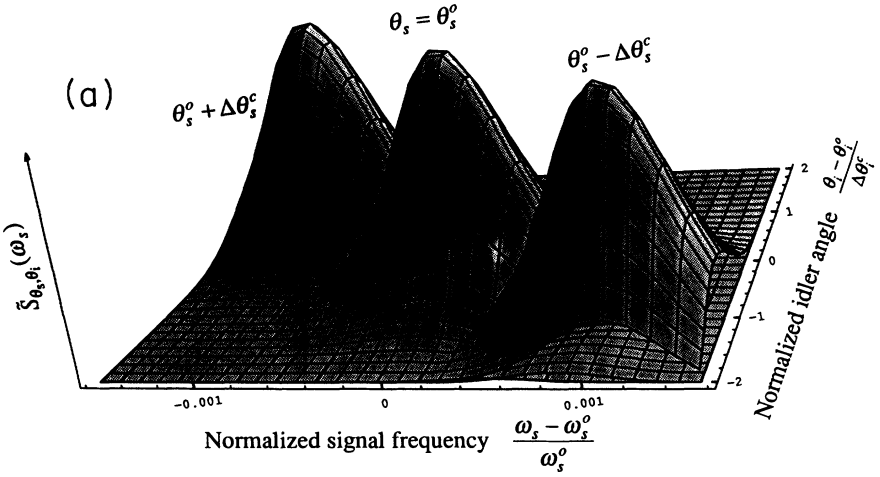

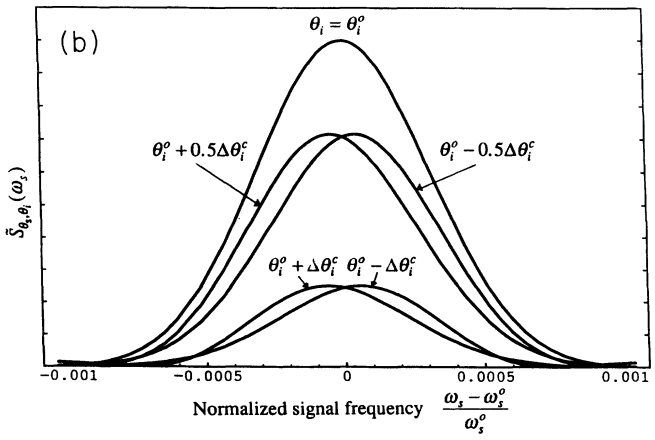

FIG. 4. (a) $\tilde{S}_{\theta_s,\theta_i}(\omega_s)$, the signal-idler cross-spectral density without the idler-frequency δ function, as a function of ω_s and θ_i for different values of θ_s, assuming the same parameters as in Fig. 3. From these parameters, we calculated $\Delta\theta_s^c=0.0105°$ and $\Delta\theta_i^c=0.0098°$. (b) Cross sections of $\tilde{S}_{\theta_s^0,\theta_i}(\omega_s)$ as a function of signal frequency for several different values of the idler direction.

which turns out to be independent of τ. This is a result of the assumption of perfect transverse momentum conservation, which implies a one-to-one relation between signal- and idler-frequency components given by Eq. (7). This relation makes Eq. (43) dependent on $t_n - t$ and τ, and both time dependences drop, after averaging over the random time t_n, in Eq. (44).

3. *Cross-spectral density*

The coincidence rate in Eq. (44), as seen by broadband detectors, can be written in the form

$$G_{si}^{(2)}(\theta_s,\theta_i;\tau)=\mu N^2\int_0^\infty d\omega_s\int_0^\infty d\omega_i S_{\theta_s,\theta_i}(\omega_s,\omega_i)\ , \tag{45a}$$

where

$$S_{\theta_s,\theta_i}(\omega_s,\omega_i)=\tilde{S}_{\theta_s,\theta_i}(\omega_s)\delta(\omega_i-\omega_i^0+a_1(\omega_s-\omega_s^0)+b_1(\theta_s-\theta_s^0)+c_1(\theta_i-\theta_i^0))\ , \tag{45b}$$

and

$$\tilde{S}_{\theta_s,\theta_i}(\omega_s)=\mu N^2\mathrm{sinc}^2\left[\frac{l}{2\pi}\{a_2(\omega_s-\omega_s^0)+b_2(\theta_s-\theta_s^0)+c_2(\theta_i-\theta_i^0)\}\right]$$
$$\times A^2(\omega_p^0+(1+a_1)(\omega_s-\omega_s^0)+b_1(\theta_s-\theta_s^0)+c_1(\theta_i-\theta_i^0))\ . \tag{45c}$$

Thus $S_{\theta_s,\theta_i}(\omega_s,\omega_i)$, the cross-spectral density, represents the coincidence rate as seen by a pair of narrowband detectors collecting light from the signal and idler directions θ_s and θ_i and centered at the frequencies ω_s and ω_i. This cross-spectral density is not equal to the product of the signal and idler spectral densities because of the entangled nature of the twin state. Also, by integrating this cross-spectral density over the idler frequencies we do not obtain the signal spectral density given in Eq. (32), but only the portion of it that is correlated with the given idler direction. To get the signal spectral density (marginal density), we need to integrate Eq. (45b) over both idler frequencies and directions, as illustrated in Fig. 2.

For a Gaussian pump, Eq. (45c) reduces to

$$\tilde{S}_{\theta_s,\theta_i}(\omega_s)=\mu N^2\exp\left[-\frac{\{\omega_s-\bar{\omega}_1(\theta_s,\theta_i)\}^2}{2\sigma_1^2}\right]$$
$$\times\mathrm{sinc}^2\left[\frac{\omega_s-\bar{\omega}_2(\theta_s,\theta_i)}{\sigma_2}\right]\ , \tag{46}$$

where $\bar{\omega}_1(\theta_s,\theta_i)$, $\bar{\omega}_2(\theta_s,\theta_i)$, σ_1, and σ_2 are given by Eqs. (35b), (35c), (35d), and (35e), respectively. The cross-spectral density is very sensitive to the pair of signal and idler directions. For a given signal direction θ_s, the intensity correlation is maximum at the matched idler direction θ_i^c given by Eq. (36). The idler entanglement angle, representing the angular width of idler directions that have a significant coincidence with the signal in the given direction, is estimated by

$$\Delta\theta_i^c\equiv|\theta_i^{+-}-\theta_i^{-+}|=\left|\frac{a_2\Delta\omega_p+(1+a_1)\frac{2\pi}{l}}{c_1a_2-c_2(1+a_1)}\right|\ , \tag{47}$$

where θ_i^{+-} and θ_i^{-+} are solutions to $\bar{\omega}_1(\theta_s,\theta_i)\pm\Delta\omega_p/(1+a_1)=\bar{\omega}_2(\theta_s,\theta_i)\pm 2\pi/a_2 l$. A similar expression for the signal entanglement angle can be obtained. In Fig. 4(a), $\tilde{S}_{\theta_s,\theta_i}(\omega_s)$ obtained from Eq. (46) is shown as a function of the normalized signal frequency and normalized idler angle for different values of signal angle θ_s. Figure 4(b) shows cross sections of $\tilde{S}_{\theta_s,\theta_i}(\omega_s)$ as a function of normalized signal frequency for different values of θ_i and for $\theta_s=\theta_s^0$.

In the limit of a monochromatic pump, Eq. (45b) reduces to

$$S_{\theta_s,\theta_i}(\omega_s,\omega_i)=2\pi\mu N^2\mathrm{sinc}^2\left[\frac{(\theta_s-\theta_s^0)}{\Delta\theta_s^c}+\frac{(\theta_s-\theta_s^0)}{\Delta\theta_i^c}\right]\delta\left[\omega_s-\omega_s^0+\frac{b_1}{(1+a_1)}(\theta_s-\theta_s^0)+\frac{c_1}{(1+a_1)}(\theta_i-\theta_i^0)\right]$$
$$\times\delta\left[\omega_i-\omega_i^0-\frac{b_1}{(1+a_1)}(\theta_s-\theta_s^0)-\frac{c_1}{(1+a_1)}(\theta_i-\theta_i^0)\right]\ , \tag{48a}$$

where

$$\Delta\theta_s^c=\left|\frac{1+a_1}{b_2(1+a_1)-b_1a_2}\right|\frac{2\pi}{l}\ , \tag{48b}$$

and

$$\Delta\theta_i^c = \left| \frac{1+a_1}{c_2(1+a_1)-c_1a_2} \right| \frac{2\pi}{l} . \tag{48c}$$

In this special case, the cross-spectral density contains a product of two δ functions that determine the frequencies in terms of the observation directions with $\omega_s+\omega_i=\omega_p^0$. The weighting factor in Eq. (48a) is determined by the sinc function representing the phase mismatch of the corresponding wave vectors.

In the opposite limit of exact phase conservation, Eq. (45b) reduces to

$$\begin{aligned} S_{\theta_s,\theta_i}(\omega_s,\omega_i) = 2\pi\mu N^2 \exp\left[-\left[\frac{(\theta_s-\theta_s^0)}{\sqrt{2}\Delta\theta_s^c} + \frac{(\theta_i-\theta_i^0)}{\sqrt{2}\Delta\theta_i^c} \right]^2 \right] \\ \times \delta\left[\omega_s-\omega_s^0+\frac{b_2}{a_2}(\theta_s-\theta_s^0)+\frac{c_2}{a_2}(\theta_i-\theta_i^0) \right] \\ \times \delta\left[\omega_i-\omega_i^0-\frac{a_2b_1-a_1b_2}{a_2}(\theta_s-\theta_s^0)-\frac{a_2c_1-a_1c_2}{a_2}(\theta_i-\theta_i^0) \right] , \end{aligned} \tag{49a}$$

where

$$\Delta\theta_s^c = \Delta\omega_p \left| \frac{a_1}{b_1a_2-b_2(1+a_1)} \right| , \tag{49b}$$

and

$$\Delta\theta_i^c = \Delta\omega_p \left| \frac{a_2}{c_1a_2-c_2(1+a_1)} \right| . \tag{49c}$$

In this special case, the correlated cross-spectral density is also a product of two δ functions that determine the frequencies in terms of the observation directions. The weighting factor in Eq. (49a) is determined by the pump amplitude at $\omega_p=\omega_s+\omega_i$, where $\omega_p-\omega_p^0$ is expressed in terms of the signal and idler angles.

C. Coincidence rates of photons collected through finite apertures

When the down-converted light is collected by slit apertures of widths $\Delta\theta_s$ and $\Delta\theta_i$ centered at θ_s^0 and θ_i^0 and in the x-z plane, the observed intensity correlation function is obtained from Eq. (44):

$$\begin{aligned} G_{si}^{(2)}(\tau) = \mu N^2 \int_{\Delta\theta_s} d\theta_s \int_{\Delta\theta_i} d\theta_i \int_0^\infty d\omega_s \operatorname{sinc}^2\left[\frac{l}{2\pi}\{a_2(\omega_s-\omega_s^0)+b_2(\theta_s-\theta_s^0)+c_2(\theta_i-\theta_i^0)\} \right] \\ \times A^2(\omega_p^0+(1+a_1)(\omega_s-\omega_s^0)+b_1(\theta_s-\theta_s^0)+c_1(\theta_i-\theta_i^0)) . \end{aligned} \tag{50}$$

On the other hand, the intensity falling on the signal aperture is obtained from Eq. (31):

$$\begin{aligned} I_s = \mu N^2 \int_{\Delta\theta_s} d\theta_s \int d\theta_i \int_0^{+\infty} d\omega_s \operatorname{sinc}^2\left[\frac{l}{2\pi}\{a_2(\omega_s-\omega_s^0)+b_2(\theta_s-\theta_s^0)+c_2(\theta_i-\theta_i^0)\} \right] \\ \times A^2(\omega_p^0+(1+a_1)(\omega_s-\omega_s^0)+b_1(\theta_s-\theta_s^0)+c_1(\theta_i-\theta_i^0)) . \end{aligned} \tag{51}$$

The intensity falling on the idler aperture I_i is given by a similar expression.

From Eqs. (50) and (51), it is apparent that the normalized intensity correlation $g_{si}^{(2)}(\tau)$ defined by

$$g_{si}^{(2)}(\tau) \equiv \frac{G_{si}^{(2)}(\tau)}{I_sI_i} \tag{52}$$

is inversely proportional to the pump intensity through the factor $1/\mu$. This behavior has been predicted and tested experimentally by Friberg, Hong, and Mandel [33].

The only distinction between Eqs. (50) and (51) is that the integral over the idler directions in Eq. (50) is restricted by the idler aperture $\Delta\theta_i$. If the idler aperture $\Delta\theta_i$ permits all directions matched to the signal aperture, then [6]

$$G_{si}^{(2)} = I_s . \tag{53}$$

This equality, modified by the signal- and idler-channel collection efficiencies, has been used to test the entangled nature of down-converted light [7] and was proposed as a technique to achieve the absolute calibration of photodetectors [34,22]. To investigate this asymptotic equality

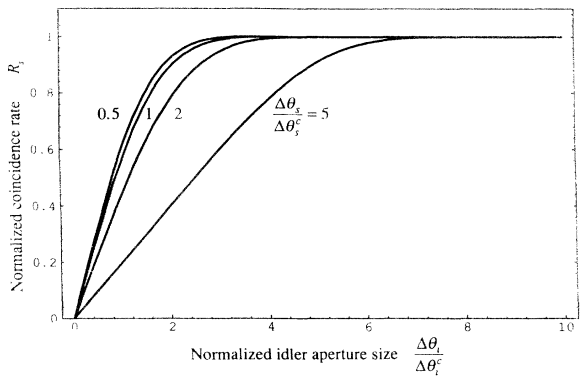

FIG. 5. Normalized coincidence rate R_s, given by Eq. (54), as a function of idler aperture for different values of signal aperture. The signal and idler aperture are assumed to be centered about the angles θ_s^0 and θ_i^0, respectively.

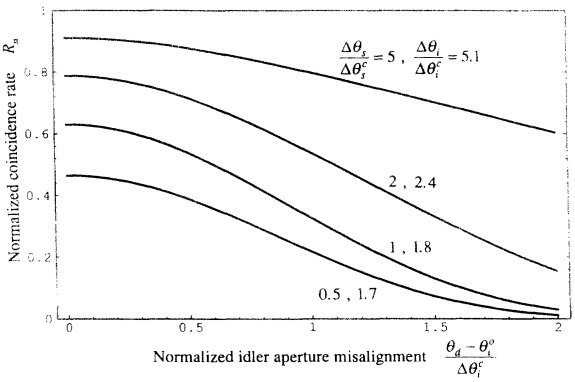

FIG. 7. Effect of idler aperture misalignment on the coincidence rate R_{si} for different signal apertures, assuming an optimal idler aperture for each case. The quantity $\theta_d-\theta_i^0$ is the idler aperture misalignment angle.

further, we examine the ratio of the coincidence rate to the signal singles rate,

$$R_s \equiv \frac{G_{si}^{(2)}}{I_s} . \tag{54}$$

This ratio is plotted in Fig. 5 for the same set of parameters used in Fig. 3, as a function of the idler aperture $\Delta\theta_i$ for different values of the signal aperture $\Delta\theta_s$.

In some applications, it is useful to normalize the coincidence rate to both the signal and idler singles rates by defining

$$R_{si} \equiv \frac{G_{si}^{(2)}}{\sqrt{I_s I_i}} . \tag{55}$$

This normalization is more appropriate when it is desired to optimize the coincidence rate for given signal and idler rates. This version of the normalized coincidence rate is shown in Fig. 6 as a function of the idler aperture $\Delta\theta_i$,

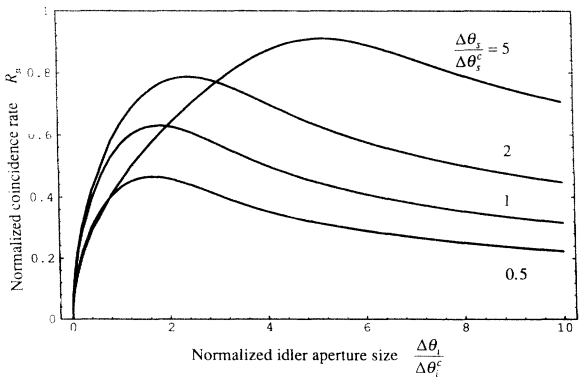

FIG. 6. Another version of the normalized coincidence rate R_{si} given by Eq. (55) as a function of idler aperture for different values of signal aperture. The signal and idler apertures are assumed to be centered about the directions θ_s^0 and θ_i^0, respectively.

for different values of the signal aperture $\Delta\theta_s$. In this case, for a given signal aperture $\Delta\theta_s$, there is an optimal idler aperture for which R_{si} is maximized. The maximum value approaches 1 for $\Delta\theta_s \gg \Delta\theta_s^c$. It is also clear from Fig. 6 that for a signal aperture $\Delta\theta_s$ smaller or of the order of the signal entanglement angle $\Delta\theta_s^c$, the optimal idler aperture $\Delta\theta_i$ is greater than the idler entanglement angle $\Delta\theta_i^c$. On the other hand, for $\Delta\theta_s \gg \Delta\theta_s^c$, the optimal idler aperture $\Delta\theta_i$ approaches the value $\Delta\theta_i^c(\Delta\theta_s/\Delta\theta_s^c)$.

The effect of misalignment of one of the apertures with respect to the other will not change the signal and idler intensities in the linear approximation used here, but it will reduce the coincidence rate. In Fig. 7, R_{si} is shown as a function of the angular misalignment of the optimal idler aperture for different signal apertures. This quantitatively accounts for the parameter ρ introduced by Larchuk *et al.* [16] to account for a reduction of fourth-order bandwidths relative to those of second order.

IV. SUMMARY AND CONCLUSIONS

The signal and idler fields generated in optical parametric down-conversion have unique spatiotemporal statistical properties, which are engendered by the energy- and momentum-matching requirements for efficient interaction. Each spectral component of the signal has a corresponding idler component for which energy matching is perfectly satisfied. Likewise, each signal plane-wave component associated with a given direction (spatial Fourier component) has an idler plane-wave component in a corresponding direction for which momentum (or phase) is perfectly matched. We have investigated the effect of imperfect phase matching by assuming a crystal of finite width, and we have assumed that the pump has a finite spectral width, so that there is more than one possibility for satisfying energy matching.

We have examined the second-order spatiotemporal coherence properties of the signal-idler field. Although the pump is spatially coherent (a plane wave), it was found that the signal- (or idler-) field plane-wave com-

ponents in different directions are statistically uncorrelated. Also, a signal-field plane-wave component is uncorrelated with any of the idler-field plane-wave components. The power spectral density associated with each plane-wave component of the signal is dependent on its direction, so that the field is not cross-spectrally pure. The center of this spectral distribution varies approximately linearly with the angle, so that it exhibits lower frequencies in one direction and higher frequencies in the other direction. The idler spectral distribution varies similarly, but in the opposite direction.

We have also determined the fourth-order (intensity) coherence functions (the photon coincidence rates) of the down-converted field as a function of the signal and idler directions. The coincidence rate for two directions within the signal is due to purely random coincidences. However, the coincidence rate for one direction within the signal and another within the idler is enhanced by the process of down-conversion. This rate is independent of the time delay τ because the correlation exists only between single frequency pairs. However, its angular dependence is governed by a cross-spectral density determined by the degree of tolerance to energy and phase mismatching, which are set by the pump spectral width and the length of the interaction region, respectively. This cross-spectral density represents the coincidence rate for each pair of signal and idler directions as seen by narrowband detectors centered at the appropriate frequencies.

Finally, we have investigated the effect of apertures on the coincidence rate normalized to the geometric mean of the signal and idler marginal rates. We have found that for a signal aperture occupying a fraction of the signal entanglement angle, the optimal normalized coincidence rate is obtained for an idler aperture occupying a larger fraction of its entanglement angle. This effect is less important for apertures much larger than their respective entanglement angles. This optimal coincidence rate approaches 100% as the matched apertures become much larger than their corresponding entanglement angles. This effect can be used to experimentally estimate the entanglement angles. The optimal coincidence rate drops gradually as the idler aperture misalignment angle exceeds the idler entanglement angle. As expected, this effect is more pronounced for small apertures.

ACKNOWLEDGMENTS

This work was supported in part by the Joint Services Electronics Program through the Columbia Radiation Laboratory and by the Office of Naval Research under Grant No. N00014-93-1-0547.

[1] T. G. Giallorenzi and C. L. Tang, Phys. Rev. **166**, 225 (1968).
[2] D. A. Kleinman, Phys. Rev. **174**, 1027 (1968).
[3] B. R. Mollow, Phys. Rev. A **8**, 2684 (1973).
[4] D. N. Klyshko, Zh. Eksp. Teor. Fiz. **83**, 1313 (1982) [Sov. Phys. JETP **56**, 753 (1982)].
[5] R. Graham, Phys. Rev. Lett. **52**, 117 (1984).
[6] C. K. Hong and L. Mandel, Phys. Rev. A **31**, 2409 (1985).
[7] D. C. Burnham and D. L. Weinberg, Phys. Rev. Lett. **25**, 84 (1970).
[8] S. Friberg, C. K. Hong, and L. Mandel, Phys. Rev. Lett. **54**, 2011 (1985).
[9] C. K. Hong and L. Mandel, Phys. Rev. Lett. **56**, 58 (1986).
[10] R. Ghosh, C. K. Hong, Z. Y. Ou, and L. Mandel, Phys. Rev. A **34**, 3962 (1986).
[11] Z. Y. Ou and L. Mandel, Phys. Rev. Lett. **61**, 54 (1988).
[12] J. G. Rarity and P. R. Tapster, J. Opt. Soc. Am. B **6**, 1221 (1989).
[13] M. A. Horne, A. Shimony, and A. Zeilinger, Phys. Rev. Lett. **62**, 2209 (1989).
[14] J. G. Rarity, P. R. Tapster, E. Jakeman, T. S. Larchuk, R. A. Campos, M. C. Teich, and B. E. A. Saleh, Phys. Rev. Lett. **65**, 1348 (1990).
[15] X. Y. Zou, T. P. Grayson, and L. Mandel, Phys. Rev. Lett. **69**, 3041 (1992).
[16] T. S. Larchuk, R. A. Campos, J. G. Rarity, P. R. Tapster, E. Jakeman, B. E. A. Saleh, and M. C. Teich, Phys. Rev. Lett. **70**, 1603 (1993).
[17] Z. Y. Ou, Phys. Rev. A **37**, 1607 (1988).
[18] Z. Y. Ou and L. Mandel, Phys. Rev. Lett. **61**, 50 (1988).
[19] J. G. Rarity, P. R. Tapster, and E. Jakeman, Opt. Commun. **62**, 201 (1987).
[20] P. R. Tapster, J. G. Rarity, and J. S. Satchell, Phys. Rev. A **37**, 2963 (1988).
[21] A. K. Ekert, J. G. Rarity, P. R. Tapster, and G. M. Palma, Phys. Rev. Lett. **69**, 1293 (1992).
[22] P. G. Kwiat, A. M. Steinberg, R. Y. Chiao, P. H. Eberhard, and M. D. Petroff, Phys. Rev. A **48**, R867 (1993).
[23] T. P. Grayson and G. A. Barbosa, Phys. Rev. A **49**, 2948 (1994).
[24] Z. Y. Ou, L. J. Wang, and L. Mandel, Phys. Rev. A **40**, 1428 (1989).
[25] R. A. Campos, B. E. A. Saleh, and M. C. Teich, Phys. Rev. A **42**, 4127 (1990).
[26] D. N. Klyshko, *Photons and Nonlinear Optics* (Gordon and Breach, New York, 1988) (translated from Russian by Y. Sviridov).
[27] L. Mandel, Phys. Rev. **144**, 1071 (1966).
[28] M. C. Teich, B. E. A. Saleh, and J. Perina, J. Opt. Soc. Am. B. **1**, 366 (1984).
[29] L. J. Wang, X. Y. Zou, and L. Mandel, Phys. Rev. A **44**, 4614 (1991).
[30] Z. Y. Ou, L. J. Wang, X. Y. Zou, and L. Mandel, Phys. Rev. A **41**, 1597 (1990).
[31] L. J. Wang, X. Y. Zou, and L. Mandel, J. Opt. Soc. Am. B **8**, 978 (1991).
[32] D. F. Edwards and R. H. White, in *Handbook of Optical Constants of Solids II,* edited by E. D. Palik (Academic, New York, 1991).
[33] S. Friberg, C. K. Hong, and L. Mandel, Opt. Commun. **54**, 311 (1985).
[34] D. N. Klyshko, Kvant. Elektron. (Moscow) **7**, 1932 (1980) [Sov. J. Quantum Electron. **10**, 1112 (1980)].

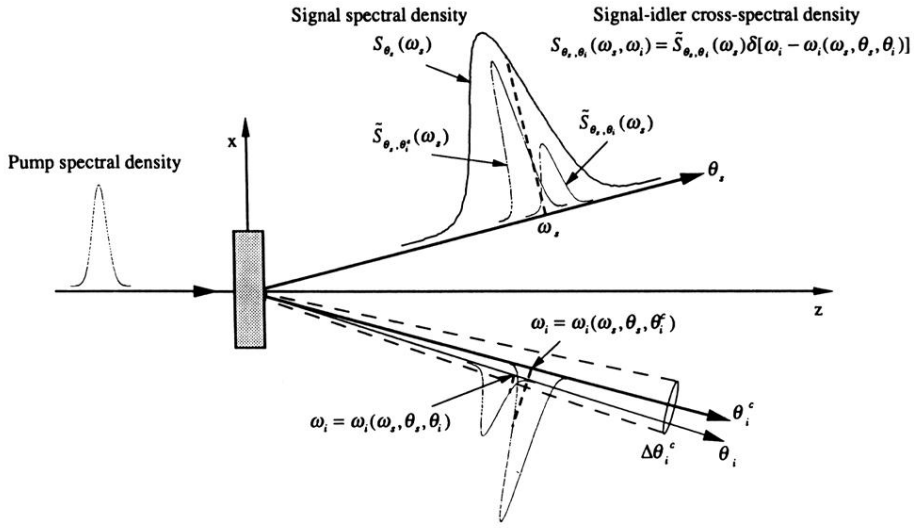

FIG. 2. Illustration of the signal spectral density and signal-idler cross-spectral density. Contributions to the signal spectral density $S_{\theta_s}(\omega_s)$ from the matched idler angle θ_i^c and from another idler angle θ_i within the idler entanglement angle $\Delta\theta_i^c$ are shown. The signal-idler cross-spectral density $S_{\theta_s,\theta_i}(\omega_s,\omega_i)$ between the pair of signal and idler directions θ_s and θ_i is given by the product of $\tilde{S}_{\theta_s,\theta_i}(\omega_s)$ and $\delta(\omega_i-\{\omega_i^0+a_1(\omega_s-\omega_s^0)+b_1(\theta_s-\theta_s^0)+c_1(\theta_i-\theta_i^0)\})$.

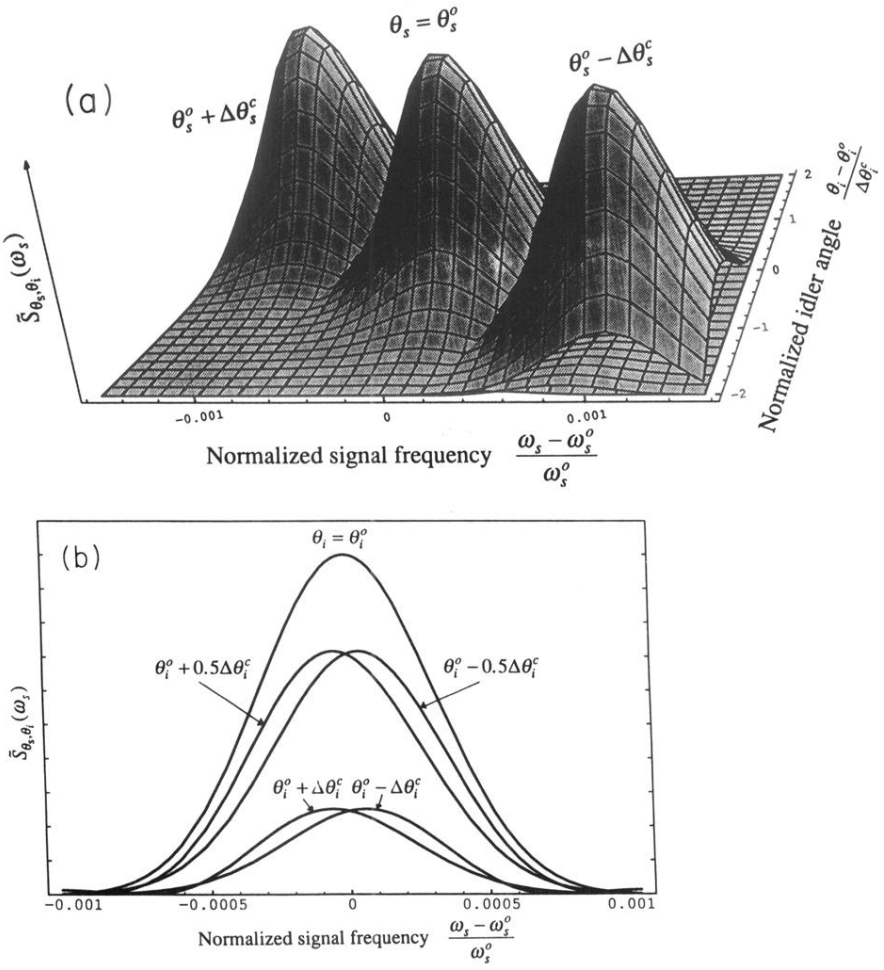

FIG. 4. (a) $\tilde{S}_{\theta_s,\theta_i}(\omega_s)$, the signal-idler cross-spectral density without the idler-frequency δ function, as a function of ω_s and θ_i for different values of θ_s, assuming the same parameters as in Fig. 3. From these parameters, we calculated $\Delta\theta_s^c = 0.0105°$ and $\Delta\theta_i^c = 0.0098°$. (b) Cross sections of $\tilde{S}_{\theta_s^0,\theta_i}(\omega_s)$ as a function of signal frequency for several different values of the idler direction.